REPORT DOCUMENTATION PAGE

Form Approved
OMB No. 0704-0188

1. REPORT DATE *(DD-MM-YYYY)*	2. REPORT TYPE	3. DATES COVERED *(From - To)*
21-07-2005	Final	July 1, 2003 - April 30, 2005

4. TITLE AND SUBTITLE

Aggregation Effects on Structures and Optical Properties of Push-Pull Chromophores:

Characterization of New Materials for Photovoltaic Thin Films: Aggregation Phenomena in Self-Assembled Perylene-Based Diimides

5a. CONTRACT NUMBER

5b. GRANT NUMBER
N00014-02-1-0584

5c. PROGRAM ELEMENT NUMBER

6. AUTHOR(S)
Daniel A. Higgins
Aifang Xie
Bei Liu

5d. PROJECT NUMBER

5e. TASK NUMBER

5f. WORK UNIT NUMBER

7. PERFORMING ORGANIZATION NAME(S) AND ADDRESS(ES)
Dept. of Chemistry
Kansas State University
Manhattan, KS 66506

8. PERFORMING ORGANIZATION REPORT NUMBER

9. SPONSORING/MONITORING AGENCY NAME(S) AND ADDRESS(ES)

10. SPONSOR/MONITOR'S ACRONYM(S)

11. SPONSOR/MONITOR'S REPORT NUMBER(S)

12. DISTRIBUTION/AVAILABILITY STATEMENT
Approved for Public Release; Distribution is Unlimited.

13. SUPPLEMENTARY NOTES

14. ABSTRACT

Under this grant, a new class of organic photovoltaic materials have been developed and characterized. These materials are comprised of cationic symmetrically- and asymmetrically-substituted perylene diimides and oppositely charged poly(acrylate) polyanions. Thin films of these materials yield photovoltages of > 140 mV for ca 0.6 W/cm2 illumination intensities, when incorporated into rudimentary heterojunction devices. Solution phase fluorescence spectra obtained from the complexes exhibit excimer-like emission and evidence of weakly coupled ground-state aggregates. Small-angle X-ray diffraction indicates the films incorporate planar bilayers of the diimide and polyanion having 3.9 nm repeat distances. Scanning probe microscopy images show the films are heterogeneous, and are comprised of sub-micrometer sized clusters that incorporate the diimide. Polarization-dependent optical imaging studies prove the perylene chromophores are semi-organized in these clusters. Application of an electric field across the films induces a depth-dependent change in the fluorescence. This effect is attributed to reorientation of the perylene chromophores under the influence of the applied field.

15. SUBJECT TERMS
Organic Photovoltaics, Polymer-Surfactant Composites, Optical Microscopy

16. SECURITY CLASSIFICATION OF:			17. LIMITATION OF ABSTRACT	18. NUMBER OF PAGES	19a. NAME OF RESPONSIBLE PERSON
a. REPORT	b. ABSTRACT	c. THIS PAGE		16	Daniel A. Higgins
					19b. TELEPHONE NUMBER *(Include area code)* (785) 532-6371

Standard Form 298 (Rev. 8/98)
Prescribed by ANSI Std. Z39.18

Final Report

Characterization of New Materials for Photovoltaic Thin Films: Aggregation Phenomena in Self-Assembled Perylene-Based Diimides

Daniel A. Higgins, P.I.
Dept. of Chemistry, Kansas State University

Grant# N00014-02-1-0584
[Original title: "Aggregation Effects on Structures and Nonlinear Optical Properties of Push-Pull Chromophores" Anne M. Kelley – Original P.I.]

Abstract

Under this grant, a new class of organic photovoltaic materials have been developed and characterized. These materials are comprised of cationic symmetrically- and asymmetrically-substituted perylene diimides and oppositely charged poly(acrylate) polyanions. Thin films of these materials yield photovoltages of > 140 mV for ≈ 0.6 W/cm^2 illumination intensities, when incorporated into rudimentary heterojunction devices. Solution phase fluorescence spectra obtained from the complexes exhibit excimer-like emission and evidence of weakly coupled ground-state aggregates. Small-angle X-ray diffraction indicates the films incorporate planar bilayers of the diimide and polyanion having 3.9 nm repeat distances. Scanning probe microscopy images show the films are heterogeneous, and are comprised of sub-micrometer sized clusters that incorporate the diimide. Polarization-dependent optical imaging studies prove the perylene chromophores are semi-organized in these clusters. Application of an electric field across the films induces a depth-dependent change in the fluorescence. This effect is attributed to reorientation of the perylene chromophores under the influence of the applied field.

1. Introduction

Perylene diimides are important organic building blocks that are currently being investigated for use in organic photovoltaics. They are most often used as the electron-transporting (or n-doped) phase in organic heterojunction devices (i.e. solar-cells).[1-12] Few alternative n-doped organic semiconductors exist. Their utility in such devices arises in part from the ease by which they can be chemically, photochemically, or electrochemically reduced (they can also be oxidized).[8,13-15] It is also important that a range of chemically-distinct diimides can be prepared from different starting amines, allowing for their solubility, film-forming capabilities and liquid crystallinity to be controlled.[11]

Thin films of controlled morphology and organization are required for applications of these materials as photovoltaics. In the past, thin film deposition has usually involved energy/equipment intensive methods like vapor deposition,[1,4,13,16] or solution-based methods such as spin casting or drop casting,[11,17,18] self-assembly,[19-22] Langmuir-Blodgett techniques,[23] or electrochemical methods.[24] The infrastructure required for vapor deposition precludes use of such methods for preparing large-area photovoltaics. Solvent casting is better in this respect,

however the use of large quantities of organic solvents can present significant economic and/or environmental challenges.

Under this grant, we initiated an entirely new research program[25] directed towards the development of new water-soluble organic semiconductors that could (in the future) simply be painted onto suitable substrates or arbitrary size and shape for solar-energy conversion applications. To this end, water-soluble, amphiphilic perylene diimides have been successfully synthesized and used in the preparation of photoactive polyelectrolyte/perylene-diimide composites that can be cast as thin films.[25] Importantly, these materials yield photocurrents and photovoltages when incorporated in rudimentary photovoltaic devices.

Figure 1 depicts the chemical structures of some of the compounds we have produced. To date, we have used them in complexes formed primarily with sodium poly(acrylate). When two aqueous solutions of the perylene diimide and poylanion are mixed, they form a water insoluble product that precipitates in time. The complex appears to be highly insoluble in a range of solvents, therefore allowing for robust, permanent films to be prepared.

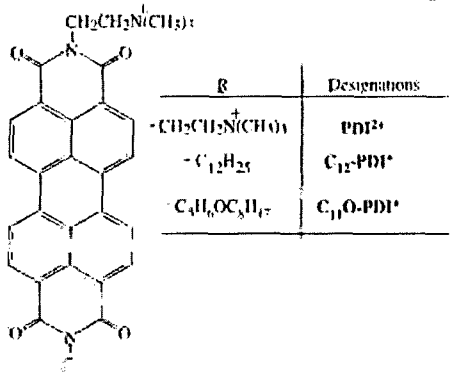

Figure 1. Example structures of the perylene diimides synthesized. A variety of alkane groups (R) have been incorporated to better control their solubility, aggregate and film-forming properties, liquid crystallinity, etc.

We are now characterizing the properties of these thin films by a number of different experimental methods, including X-ray diffraction (to assess molecular organization), electrochemistry (to determine their oxidation/reduction potentials), fluorescence and UV-vis absorption spectroscopies (to observe aggregation phenomena and determine electronic transition energies), atomic force microscopy (to characterize surface morphology and film structure), near-field scanning optical microscopy (NSOM) and multiphoton-excited fluorescence microscopy (MPEFM) (these last two allow for a better understanding of their submicrometer optical properties, film structure, local chromophore organization, and charge carrier dynamics). We recently reported our initial results on these materials in a full-length article in the journal *Langmuir*.[25]

2. Sample Preparation

A number of symmetrically- and asymmetrically-substituted perylene diimides were synthesized under this grant. Examples of the compounds produced are depicted in Figure 1. The development of efficient procedures for the synthesis of the asymmetric compounds required the extensive efforts of a postdoc and an undergraduate student, working over a period of several months. Synthesis of the alkane-based asymmetric compounds was made difficult by well-

known solubility limitations of the starting materials and products. Nevertheless, we can now easily obtain pure compounds in ca 100 mg quantities as needed. Significant improvement in the ease of synthesis was obtained by the use of ether-based[11] hydrophilic tail groups in more recent work.

Perylene diimide/polyelectrolyte composites were then prepared by mixing aqueous solutions (ca 100 μM) of the various perylene diimides and polyelectrolyte (sodium poly(acrylate), or PA^-). Sub-stoichiometric complexes were found to remain in solution for long periods of time, whereas near stoichiometic complexes (> 1:2 C_n-PDI^+:PA^-) tended to precipitate over a few hours. Stoichiometric complexes precipitated almost immediately. Such results are of course dependent on solution ionic strength.

All films employed were prepared by drop casting the composites directly onto glass or ITO-coated glass slides. The films were then dried in an oven for several hours. Such methods yield relatively rough films comprised of large aggregated structures. We are now investigating solvent vapor annealing[10] as a means to better control film properties, and will also explore sequential (layer-by-layer) deposition procedures[26] as a means to prepare more well-ordered layered structures. In the future, we plan to investigate solution spray coating methods as a means to prepared large area devices.

Films for NSOM and some MPEFM experiments were cast alone on microscope cover slips and/or ITO-coated cover slips. For the production of rudimentary photovoltaic devices and for some MPEFM studies, layered structures were prepared. In these devices, TPD (a well-known hole conductor)[27] was solvent cast (from chloroform) either onto the ITO slide or on C_n-PDI^+/PA^- coated ITO. A second electrode (i.e. Al, Ag, or In) was then vapor deposited on top. Some samples were also prepared between two ITO-coated substrates. In these, a layer of optical epoxy was added to ensure good connection between the electrodes and the sample and to serve as a charge-blocking layer. In some instances (i.e, in electric field studies [see below]), insulating layers of SiO were also employed as additional charge-blocking layers and were appropriately deposited onto the ITO slides directly.

3. Bulk Sample Characterization

p-n Heterojunction Devices

The possible utility of the C_n-PDI^+/PA^- composites as alternative organic semiconducting/photovoltaic materials was assessed by preparing and testing rudimentary p-n heterojunction devices. These devices usually consisted of an ITO coated glass slide onto which a thin film of the C_n-PDI^+/PA^- composite (serving as the n-type material) and TPD were cast and dried. Each of the organic films was ≈ 2 μm thick. The films were then coated with either silver, aluminum, or indium to form the second electrode. After electrical connections were made to the device, the metal side was isolated from the ambient atmosphere using optical epoxy. Under illumination with 488 nm light (≈ 0.6 W/cm^2), these devices exhibited open-circuit photovoltages of > 140 mV. However, it often took several minutes of exposure for these photovoltages to develop. These samples also exhibited diode-like I-V curves. Figure 2 shows representative I-V curves obtained in the dark and under 488 nm illumination. Unfortunately, they have only yielded sub-optimal photocurrent characteristics to date, and do not exhibit the same photovoltages as measured independently, above. The semiconducting properties of these materials will be explored in more detail in the future.

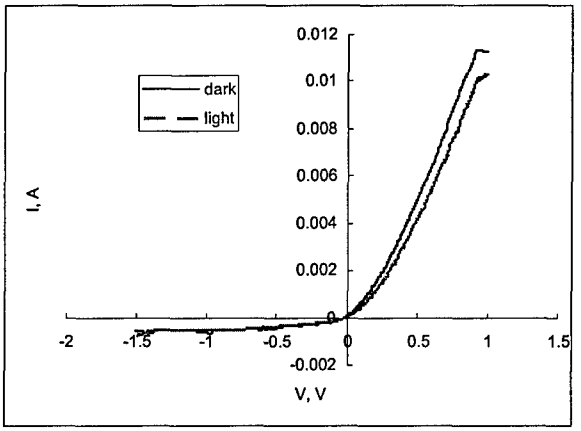

Figure 2. Representative I-V curves for a rudimentary p-n heterojunction device prepared from C_{12}-PDI^+/PA^- and TPD. ITO-coated glass and vapor-deposited silver metal comprised the electrodes.

X-ray Structural Information

Thin-film materials based on more conventional surfactants (in place of C_{12}-PDI^+) and similar polyelectrolytes exhibit a diversity of morphological structures, showing organization on relatively large (i.e. a few nanometers) length scales.[28,29] Generally, they exhibit little short range (angstrom scale) organization. They have previously been observed to form planar bilayers,[30-32] perforated or undulating bilayers,[28,30] and cubic[30,33] and hexagonal phases.[34,35] Based on these previous studies, and the planar nature of the perylene chromophore, we have hypothesized that thin films formed from our composites should incorporate planar bilayers. The perylene diimides are expected to form "π-stacks" within the bilayers, with the bilayers comprised of alternating ionic layers of the charged C_n-PDI^+ headgroups and the anionic polyelectrolyte and nonpolar regions comprised of the alkane chains of the asymmetric perylene diimides.

X-ray scattering data obtained in studies of the C_{12}-PDI^+/PA^- composite thin films are shown in Figure 3. These data were collected in both wide angle (WAXS) and small angle (SAXS) geometries. The WAXS data in all C_{12}-PDI^+/PA^- films exhibit a weak, broad peak in the $2\theta = 15\text{-}35^\circ$ range. WAXS data obtained from films of pure C_{12}-PDI^+ or pure PA^- exhibit a similar feature. Its appearance indicates the materials are disordered on short (i.e. 0.25-0.60 nm) length scales, and it may be concluded that neither the alkane chains of the C_{12}-PDI^+ molecules, nor the polymer hydrocarbon backbones are particularly ordered. It may also be concluded that the perylene chromophores, which often exhibit relatively strong π-stacking interactions, are relatively disordered.

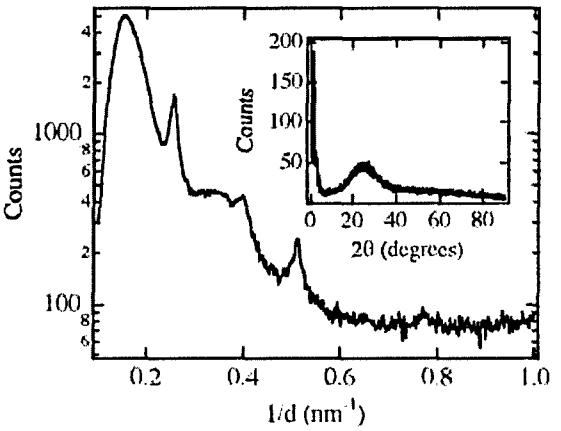

Figure 3. Small and wide (insert) angle X-ray diffraction data from a thin film of C_{12}-PDI^+/PA^- cast on a glass slide. The series of sharp peaks in the SAXS data suggest the presence of planar bilayers in the C_{12}-PDI^+ phase with 3.9 nm spacing, while the broad peak exhibited in the WAXS data indicate the materials are disordered on the angstrom scale.

In contrast to the WAXS data, the SAXS data indicate the presence of long-range organization (occurring over several nanometers) in the C_{12}-PDI^+/PA^- composites. Most noteworthy is the appearance of a series of relatively sharp peaks corresponding to multiple (up to three) orders of diffraction from a single film structural feature. Here, these diffraction peaks are attributed to the bilayers believed to be present in these films. Figure 4 shows the proposed model for C_{12}-PDI^+/PA^- composite organization. From the SAXS data, the bilayer spacing in the films is deduced to be 3.9 nm. The relatively small bilayer spacing (C_{12}-PDI^+ is calculated to be $\approx$ 3 nm in length, assuming an extended alkane chain) is most likely due to "tilting" of the C_{12}-PDI^+ species, accompanied by significant interdigitation of the alkane chains within the bilayers. Assuming extended alkane chains and full interdigitation, the alkane chains are still required to be tilted by $\approx 20^\circ$ to form bilayers with 3.9 nm repeat distances, as shown in Figure 4. In such a structure, the C_{12}-PDI^+ chromophores would also be tilted by $\approx 50^\circ$ from the film normal. Tilting of the chromophores leads to an offset in the π-stacking of the chromophores, and a shift in the electronic transition energies within the aggregate.

While the narrow peaks observed in the SAXS data are consistent with the presence of bilayers, the broader peaks also observed indicate that the film organization is actually more complicated. These results suggest the C_{12}-PDI^+/PA^- composites may be two dimensionally ordered, may simultaneously form two or more different polymorphs, or there may be two or more chemically distinct forms of the composite present. In fact, SAXS studies of pure C_{12}-PDI^+ films exhibit diffraction patterns very similar to the series of broad peaks depicted in Figure 3. Hence, the broad peaks are tentatively assigned to C_{12}-PDI^+ phases that do not incorporate polyelectrolyte. These "pure" C_{12}-PDI^+ structures are more disordered and less tightly packed than the relatively well-ordered composite bilayers discussed above. Their greater spacing could result from less efficient packing of the molecules brought about by enhanced electrostatic repulsion of the ionic C_{12}-PDI^+ headgroups. Unfortunately, it is not possible to determine the actual film structures in greater detail at the present time. We will address this issue in greater depth in future studies employing the series of C_n-PDI^+ compounds and/or the C_nO-PDI^+ series.

Annealing methods are also now being used to change/control composite organization; the results will provide a more concrete picture of the organization.

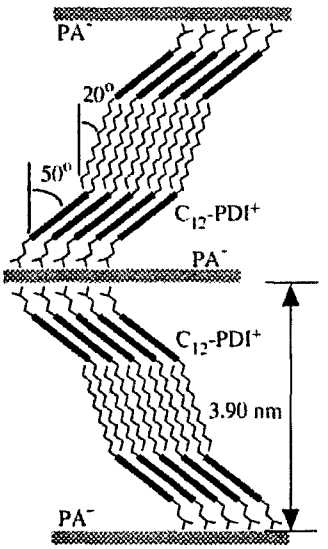

Figure 4. Proposed model for C_{12}-PDI^+ structure observed in the SAXS data (Figure 3). The thick dark lines represent the planes of the perylene diimide moeities.

In the future, the planar bilayer structures present in these materials could lead to the production of organic semiconducting films with unique 2-D charge conduction mechanisms. The presence of the ionic, hydrophilic layers are also important in that they suggest the materials should readily absorb water (although they are insoluble in water). Hence, water-vapor annealing of these structures is also possible.

Bulk Spectroscopic Data

While the X-ray data described above indicate a lack of short-range order in the C_{12}-PDI^+/PA^- composites, absorption and fluorescence spectra of the composites indicate that the chromophores are indeed aggregated, and hence, positioned in close proximity to each other. Figure 5 depicts the solution-phase UV-visible absorption, fluorescence excitation and fluorescence emission spectra obtained from a series of composites. These composites were prepared with varying polyelectrolyte concentrations to yield a series of complexes having different stoichiometries. An approximately constant ionic strength was maintained throughout.

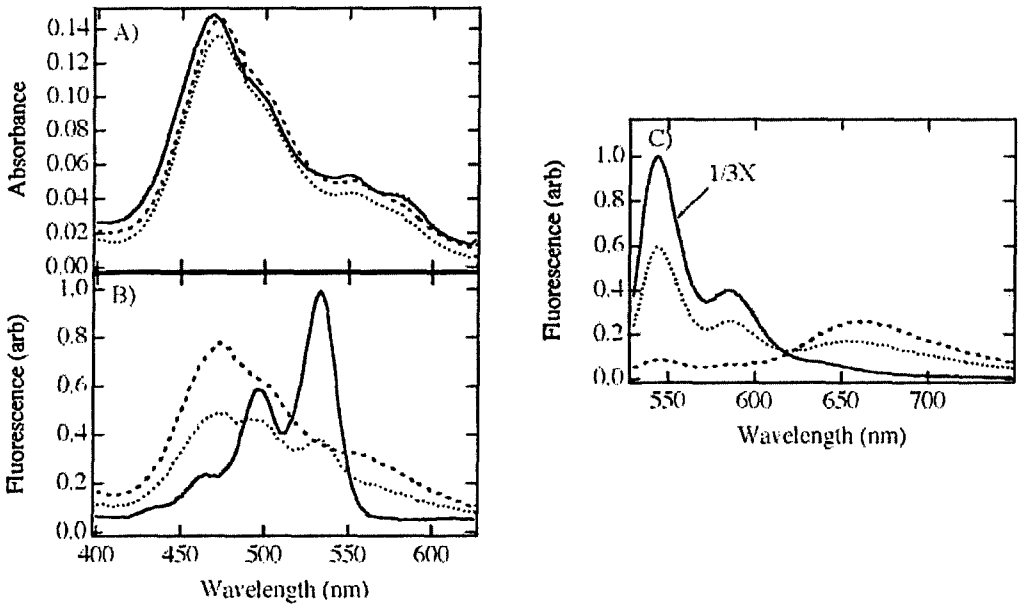

Figure 5. A) Absorbance, **B)** fluorescence excitation and **C)** fluorescence emission spectra obtained from C_{12}-PDI^+/PA^- composites in aqueous solution. The data indicate the perylene chromophores are aggregated even at very low concentrations and that weak excimer emission is observed in the presence of PA^-, suggesting a change in materials structure. The concentration of PA^- in each case is 0.0 μM (solid lines), 15 μM (dotted lines) and 30 μM (dashed lines). The concentration of C_{12}-PDI^+ is 10 μM throughout.

Even at concentrations as low as 10 μM (see Figure 5) the C_{12}-PDI^+ spectra are broadened and blue-shifted from those observed for the monomeric species in dilute ethanol solutions (not shown). In contrast, the fluorescence excitation and emission spectra of these same solutions are nearly identical to those of the monomeric species. The intensity of fluorescence from the aqueous solutions, however, is greatly decreased from that observed in the organic solvents. For example, the emission yield of C_{12}-PDI^+ is measured to be 0.73 in ethanol solution, while that measured in aqueous solution is < 0.01.

From these studies, as well as those performed on related compounds, it is concluded that the C_{12}-PDI^+ is almost completely aggregated at 10 μM concentrations in aqueous solution. The fluorescence excitation and emission spectra reflect the presence of a small amount of residual monomeric C_{12}-PDI^+ and the aggregates formed (absent PA^-) appear to be totally nonfluorescent.

Upon addition of an excess of PA^-, the emission spectrum shifts dramatically to the red (from 544 nm to 660 nm) and broadens significantly. The emission yield also drops precipitously, but the species formed remain slightly fluorescent. Figure 6 shows a series of photographs depicting the change in sample color and fluorescence as a function of PA^- concentration most dramatically. Broadened, red-shifted emission like that exhibited by the C_{12}-PDI^+/PA^- composite is usually attributed to the formation of excimers.[15] However, the blue-shifted absorption and excitation spectra that are observed suggest the C_{12}-PDI^+/PA^- complex is also aggregated in the ground-state (similarly to C_{12}-PDI^+ alone).[36] Ground state aggregates have also been observed in related (but covalently linked) perylene diimides, based on NMR studies.[37] In the present materials, it is concluded that aggregation of the chromophores in the

presence of PA^- facilitates excimer formation by positioning the chromophores in closer proximity to each other.

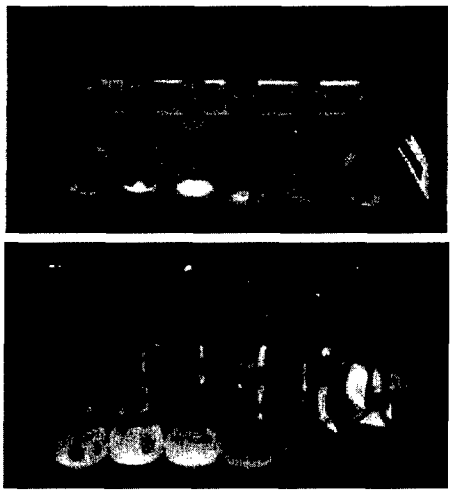

Figure 6. Top) Transmitted light photograph depicting changes in the colors of C_{12}-PDI^+/PA^- solutions as a function of PA^- concentration in aqueous solution. Bottom) Fluorescence photograph depicting changes in the fluorescence observed from these same solutions. The PA^- concentration is zero on the left and increases to the right.

The fact that excimer emission is not observed from the aqueous C_{12}-PDI^+ solutions absent PA^- indicates the polyelectrolyte plays an important role in controlling aggregate structure. Most notably, the shielding of the positive charges on the C_{12}-PDI^+ molecules by the anionic sites of the polyelectrolyte allows for the individual chromophores to more closely approach each other. Studies in which a polycation was used in place of PA^- showed no evidence of excimer emission, proving that these effects are a direct result of ionic interactions between C_{12}-PDI^+ and PA^-.

Solution-Phase Electrochemical Experiments

Cyclic voltammetry studies of C_{12}-PDI^+ and PDI^{2+} in acetonitrile show that both these compounds readily undergo two sequential one electron reductions ($E_{peak,1} \approx$ -200 mV vs NHE and $E_{peak,2} \approx$ -500 mV vs NHE). Evidence for strong adsorption of the reduced species is also depicted in the data.[38] These results are consistent with those published previously for different perylene-diimides,[14,15] indicating they should exhibit similar photoelectrochemical behavior as well.

Scanning Probe Microscopy Studies

Atomic force microscopy (AFM) and near-field scanning optical microscopy (NSOM) data have provided valuable information on film morphology in the C_n-PDI^+/PA^- composites, indicating that the films we are preparing are extremely heterogeneous, showing topographic features approaching one micrometer in size and a few micrometers in lateral dimension. Such results were not entirely unexpected, since our solution-phase investigations indicate C_n-PDI^+ and PA^- form strong complexes that frequently precipitate from solution. However, such a high degree of heterogeneity is not desirable and could be the cause of the suboptimal photovoltaic properties observed from our films to date.

At present, we are beginning to explore a number of different methods for improving film quality. These include the use of the C_nO-PDI^+ series of compounds, which are vastly more soluble than the C_n-PDI^+ series. We are also exploring methods of modifying the film structure by solvent-vapor annealing (thermal annealing experiments failed to alter the morphology of the as-prepared films). Both water-vapor and organic-vapor annealing are being explored.

Multiphoton-Excited Fluorescence Microscopy

Thin films of the C_{12}-PDI^+/PA^- composites were also characterized by multiphoton-excited fluorescence microscopy (MPEFM).[39,40] These studies provide valuable information on the film quality and overall film morphology, complementary to that obtained by the scanning probe methods. As shown in our recent publication,[25] MPEFM also provides valuable data on chromophore organization. Importantly, these microscopic results allow for direct characterization of C_{12}-PDI^+/PA^- composite organization on sub-micrometer length scales.

Figure 7 shows an MPEFM micrograph of a C_{12}-PDI^+/PA^- composite film. Here, fluorescence excitation of the perylene chromophores occurs by two photon excitation using ≈ 800 nm light.[25] These films are clearly inhomogeneous, exhibiting fluorescent structures having a broad range of sizes from several micrometers (lateral size) down to the smallest resolvable features (i.e. of diffraction limited size). We have chosen to use MPEFM in these studies over more conventional imaging methods because of its sub-diffraction-limited spatial resolution, its inherent depth selectivity (allowing for three-dimensional resolution of sample structures) and the substantially reduced background (important for imaging of weakly fluorescent sample such as the C_{12}-PDI^+/PA^- composite thin films imaged here).[39-41] The depth-resolved imaging capabilities of MPEFM are depicted in Figure 8, in which the several images have been recorded from the same film at different focus depths. Such studies allow for the heterogeneity of the films to be explored as a function of film depth. They also allow for images of different film regions (i.e. the p and n-type regions of a heterojunction device) to be separately and selectively imaged.

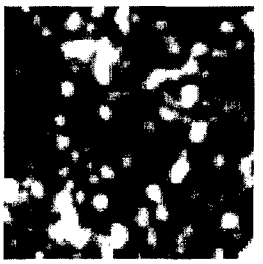

Figure 7. Representative 10x10 μm fluorescence image of a C_{12}-PDI^+/PA^- composite film recorded by MPEFM. Such images depict the dramatic heterogeneity observed in these films.

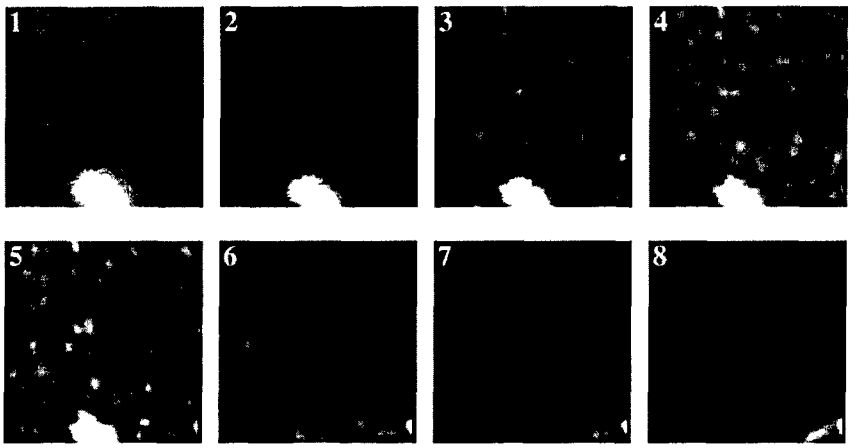

Figure 8. Depth-resolved MPEFM images of a C_{12}-PDI^+/PA^- film. This sequence of images shows the film is on average < 2 μm thick. However, there is noticeable heterogeneity in the depth dimension as well (note the "fiber" that appears in the last few images, and is "deep" within the sample).

Reconciliation of the SAXS data with the NSOM and MPEFM data indicates that the C_n-PDI^+/PA^- complexes must be organized over reasonably short length scales. Polarization-dependent MPEFM has confirmed this hypothesis,[25] showing the bright fluorescent spots observed in these images are semi-ordered. It is likely the planar bilayer structures proposed in Figure 4 are severely truncated (i.e. they only extend over a few hundred nanometers at most).

Electric-Field-Induced Fluorescence Quenching Studies

Most recently, we have been attempting microscopic, electric-field-induced fluorescence quenching experiments using MPEFM. These studies were initially begun in order to understand the influence of sample heterogeneity on charge generation and charge carrier migration in the C_n-PDI^+/PA^- composite films. The results have proven extremely challenging to interpret. As a result, a wide variety of samples with different geometries have been prepared and characterized. Especially intriguing in these studies has been the observation that in most samples an applied electric field causes apparent fluorescence quenching when the laser is focused "deep" within a sample (i.e. 1-2 μm from the surface nearest the microscope objective) but causes apparent fluorescence enhancement when focused on the near-side of the sample. We now believe this effect arises entirely from reorientation of the PDII chromophores under the influence of the applied electric field. Hence, the results reflect the mobility of the molecules, rather than charge-carrier dynamics.

Here, we emphasize only a very small subset of our experimental results to prove this point. The sample geometries employed are shown below in Figure 9. In both, sandwich devices constructed between ITO-coated substrates were employed. The ITO surfaces were coated with SiO_x (by vapor depositing SiO) to serve as charge-blocking layers. The C_n-PDI^+/PA^- composite was then deposited on one of the SiO_x-coated ITO surfaces. A layer of optical epoxy was added to serve as a charge-blocking layer and to ensure good contact between the sample and electrodes.

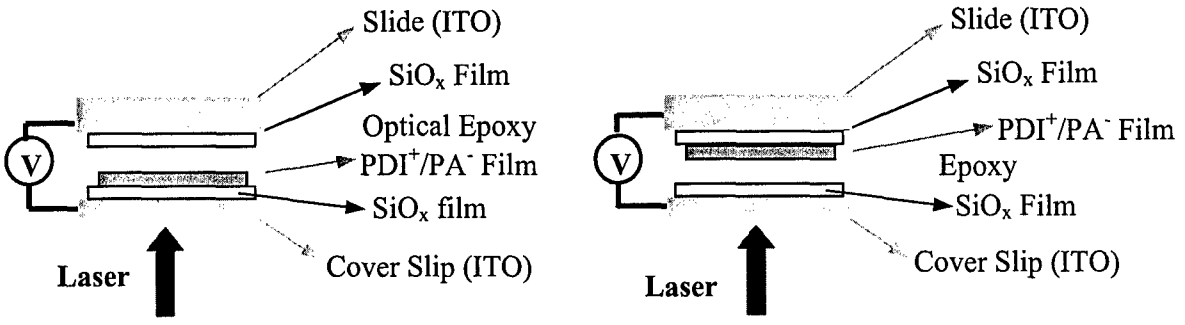

Figure 9. Sample geometries employed in the experiments described herein.

Figure 10 shows representative MPEFM time traces obtained as a function of position within the sample. In each, the fluorescence appears to be enhanced when the focus is positioned at the near-edge of the sample (closest to the microscope objective). In contrast, the fluorescence appears to be quenched when the focus is positioned further within the sample (furthest from the microscope objective). The fact that the behavior observed is identical for the two geometries shown above indicates that effect is not likely due to field-induced charge carrier generation and separation as is often described in similar experiments.[42]

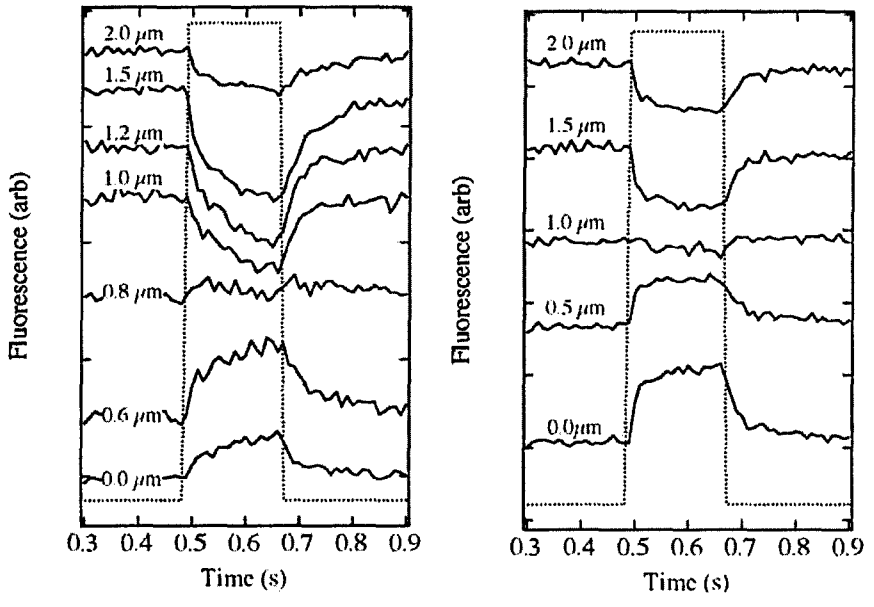

Figure 10. Depth-dependent electric-field-induced changes in the fluorescence observed from the samples shown in Figure 9. Depth into the C_n-PDI^+/PA^- film is shown on each time trace. Several of the traces have been offset in the vertical direction to allow for better display. The dashed line depicts the electric field pulse duration.

To further explore the origins of this effect, we have also performed power-dependent and field-dependent studies. Figure 11 shows the relative fluorescence signal (field on relative to field off) to be independent of incident power, indicating these effects do not arise from any nonlinear photoinduced processes. (The subtle changes observed are due to a small background signal that has not been subtracted.)

Also shown in Figure 11 are the field-dependences of the fluorescence increase/decrease (for two different depths in the sample). From these results, there appears to be a "threshold" field strength, below which no change in signal occurs. Above this "threshold", the signal changes dramatically upon application of the field. Initially, the change in signal with field strength is superlinear (scaling approximately as the square of the applied field), suggestive of a Kerr-effect mechanism. At the highest fields, the effect "saturates" and the fluorescence changes much less dramatically with increasing field strength. Importantly, for depths where decreased fluorescence is obtained in the presence of an applied field, the signal near saturation still remains far above the background level.

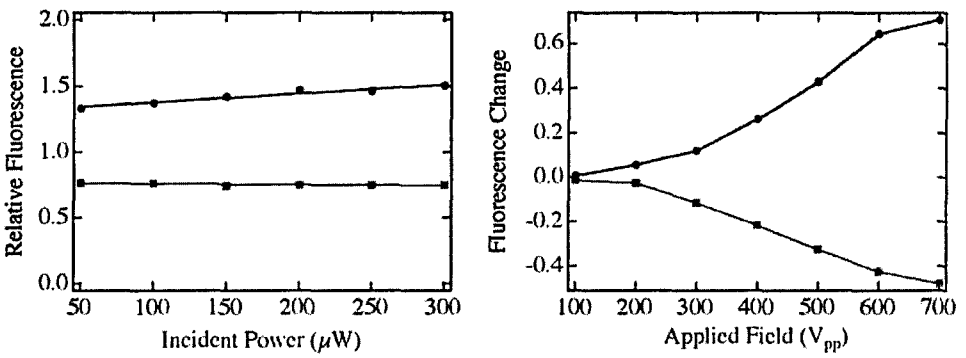

Figure 11. (Left) Fluorescence signal ("field on" relative to "field off") as a function of incident laser power from regions deep within the sample (red squares) and from the near side of the sample (blue circles) . (Right) Relative increase/decrease in the fluorescence signal as a function of applied field strength. From regions deep within the sample (red squares) and from the near side (blue circles).

These results are very similar to those we have obtained previously in field-induced reorientation studies of polymer dispersed liquid crystals.[43] As a result, we attribute the signal changes (both increase and decrease) to electric-field-induced reorientation of the C_n-PDI$^+$ chromophores. While these molecules are charged, they have little or no dipole moment. Reorientation in such cases is driven by interactions of the field with the field-induced dipole moment of the molecule (formally, a Kerr effect). Hence, the signal is indeed expected to change in a nonlinear fashion with field strength.

The observation of *both* a signal increase on the near-side of the sample and a signal decrease from deep within the sample can also be explained by the reorientation mechanism, coupled with self absorption in the sample. Molecules in the sample appear to reorient under the field so that they are more efficiently excited by the incident light. However, the emission from deep (1-2 μm) within the sample must pass back through the sample to reach the objective. Depending on the emission wavelength, some of this light is absorbed under these circumstances. The greater the reorientation of the chromophores, the greater the absorption.

Therefore, we propose that the long axis of the chromophores is reoriented closer to the plane of the sample under the influence of the field. Since the primary electronic transition involved in excitation of the molecules is polarized along the long molecular axis, reorientation may actually be driven by polarization of the aggregate (rather than individual molecules). The individual molecules are most polarizable along their long axes as well. Hence, were the molecules to interact with the field and reorient independently of each other, one would expect to see a reduction in the signal on the near side and an increase in signal from deep within the film.

The field-dependent results obtained indicate that the C_n-PDI$^+$ chromophores are somewhat mobile in these films. Such an effect suggests that these materials should be readily annealable and should exhibit somewhat dynamic order. As a result, final photovoltaic materials prepared from these samples may exhibit self-healing tendancies in which damage is automatically repaired. Photovoltaics of this sort would have extended lifetimes, reducing the overall average costs of operation.

4. Project Participants

Several graduate students, postdocs, and two undergraduate students have contributed to this project. These students have received valuable training in a number of physical methods and in organic synthesis. Their training under this grant (and under new funding obtained from NSF for a related project) will have a direct impact on the development of new human resources in the physical sciences in the U.S. The maintenance and development of new human resources in the physical sciences are of profound and absolute importance to our country's national security and are therefore of direct importance to the US Department of Defense.

Project Participants:

1) Daniel Higgins, Project Director
2) Aifang Xie, PhD, Chinese Academy of Sciences, Beijing
3) Bei Liu, PhD, Kansas State University
4) Jeffrey Hall, PhD, Kansas State University
5) Sarah Barron, BS, Kansas State University
6) Amy Twite, pursuing BS, Kansas State University

References

(1) Forrest, S. R.; Kaplan, M. L.; Schmidt, P. H.; Feldmann, W. L.; Yanowski, E. *Appl. Phys. Lett.* **1982**, *41*, 90-93.

(2) Loutfy, R. O.; Hor, A.-M.; Hsiao, C.-K.; Baranyi, G.; Kazmaier, P. *Pure Appl. Chem.* **1988**, *60*, 1047-1054.

(3) Katz, H. E.; Lovinger, A. J.; Johnson, J.; Kloc, C.; Siegrist, T.; Li, W.; Lin, Y.-Y.; Dodabalapur, A. *Nature* **2000**, *404*, 478-481.

(4) Katz, H. E.; Johnson, J.; Lovinger, A. J.; Li, W. *J. Am. Chem. Soc.* **2000**, *122*, 7787-7792.

(5) Gregg, B. A. *J. Phys. Chem. B* **2003**, *107*, 4688-4698.

(6) Wang, S.; Li, Y.; Du, C.; Shi, Z.; Xiao, S.; Zhu, D.; Gao, E.; Cai, S. *Synth. Metals* **2002**, *128*, 299-304.

(7) Giaimo, J. M.; Gusev, A. V.; Wasielewski, M. R. *J. Am. Chem. Soc.* **2002**, *124*, 8530-8531.

(8) Lukas, A. S.; Zhao, Y.; Miller, S. E.; Wasielewski, M. R. *J. Phys. Chem. B* **2002**, *106*, 1299-1306.
(9) Adams, D. M.; Kerimo, J.; Olson, E. J. C.; Zaban, A.; Gregg, B. A.; Barbara, P. F. *J. Am. Chem. Soc.* **1997**, *119*, 10608-10619.
(10) Conboy, J. C.; Olson, E. J. C.; Adams, D. M.; Kerimo, J.; Zaban, A.; Gregg, B. A.; Barbara, P. F. *J. Phys. Chem. B* **1998**, *102*, 4516-4525.
(11) Cormier, R. A.; Gregg, B. A. *Chem. Mater.* **1998**, *10*, 1309-1319.
(12) Struijk, C. W.; Sieval, A. B.; Dakhorst, J. E. J.; van Dijk, M.; Kimkes, P.; Koehorst, R. B. M.; Donker, H.; Schaafsma, T. J.; Picken, S. J.; van de Craats, A. M.; Warman, J. M.; Zuilhof, H.; Sudhölter, E. J. R. *J. Am. Chem. Soc.* **2000**, *122*, 11057-11066.
(13) Tamizhmani, G.; Dodelet, J. P.; Cote, R.; Gravel, D. *Chem. Mater.* **1991**, *3*, 1046-1053.
(14) Lee, S. K.; Zu, Y.; Herrmann, A.; Geerts, Y.; Müllen, K.; Bard, A. J. *J. Am. Chem. Soc.* **1999**, *121*, 3513-3520.
(15) Williams, M. E.; Murray, R. W. *Chem. Mater.* **1998**, *10*, 3603-3610.
(16) Schlettwein, D.; Back, A.; Schilling, B.; Fritz, T.; Armstrong, N. R. *Chem. Mater.* **1998**, *10*, 601-612.
(17) Miller, L. L.; Zhong, C.; Hong, Y. *Synth. Metals* **1994**, *62*, 71-73.
(18) Miller, L. L.; Duan, R. G.; Hong, Y.; Tabakovic, I. *Chem. Mater.* **1995**, *7*, 1552-1557.
(19) Kwan, W. S. V.; Atanasoska, L.; Miller, L. L. *Langmuir* **1991**, *7*, 1419-1425.
(20) Würthner, F.; Thalacker, C.; Sautter, A. *Adv. Mater.* **1999**, *11*, 754-758.
(21) Rodrigues, M. A.; Bemquerer, M. P.; Politi, M. J.; Brochsztain, S.; Miranda, M. T. M.; Baptista, M. S. *Chem. Lett.* **2002**, *2002*, 604-605.
(22) Schenning, A. P. H. J.; Herrikhuyzen, J. V.; Jonkheijm, P.; Chen, Z.; Würthner, F.; Meijer, E. W. *J. Am. Chem. Soc.* **2002**, *124*, 10252-10253.
(23) Antunes, P. A.; Constantino, C. J. L.; Aroca, R. F.; Duff, J. *Langmuir* **2001**, *17*, 2958-2964.
(24) Miller, L. L.; Zhong, C.-J.; Kasai, P. *J. Am. Chem. Soc.* **1993**, *1993*, 5982-5990.
(25) Xie, A.; Liu, B.; Hall, J. E.; Barron, S. L.; Higgins, D. A. *Langmuir* **2005**, *21*, 4149-4155.
(26) Cooper, T. M.; Campbell, A. L.; Crane, R. L. *Langmuir* **1995**, *11*, 2713-2718.
(27) Law, K.-Y. *Chem. Rev.* **1993**, *93*, 449-486.
(28) Antonietti, M.; Conrad, J.; Thünemann, A. *Macromolecules* **1994**, *27*, 6007-6011.
(29) MacKnight, W. J.; Ponomarenko, E. A.; Tirrell, D. A. *Acc. Chem. Res.* **1998**, *31*, 781-788.
(30) Antonietti, M.; Burger, C.; Effing, J. *Adv. Mater.* **1995**, *7*, 751-753.
(31) Ponomarenko, E. A.; Waddon, A. J.; Tirrell, D. A.; MacKnight, W. J. *Langmuir* **1996**, *12*, 2169-2172.
(32) Wenzel, A.; Antonietti, M. *Adv. Mater.* **1997**, *9*, 487-490.
(33) Antonietti, M.; Conrad, J. *Angew. Chem. Int. Ed. Engl.* **1994**, *33*, 1869-1870.
(34) Zhou, S.; Yeh, F.; Burger, C.; Chu, B. *J. Phys. Chem. B* **1999**, *103*, 2107-2112.
(35) Thünemann, A. F.; Ruppelt, D. *Langmuir* **2000**, *16*, 3221-3226.
(36) Iverson, I. K.; Casey, S. M.; Seo, W.; Tam-Chang, S.-W. *Langmuir* **2002**, *18*, 3510-3516.
(37) Wang, W.; Han, J. J.; Wang, L.-Q.; Li, L.-S.; Shaw, W. J.; Li, A. D. Q. *Nano Lett.* **2003**, *4*, 455-458.
(38) Bard, A. J.; Faulkner, L. R. *Electrochemical Methods: Fundamentals and Applications*; John Wiley and Sons, Inc.: New York, 1980.
(39) Denk, W.; Strickler, J. H.; Webb, W. W. *Science* **1990**, *248*, 73-76.
(40) Gratton, E.; Barry, N. P.; Beretta, S.; Celli, A. *Methods* **2001**, *00*, 103-110.

(41) Deitche, J.; Kempe, M.; Rudolph, W. *J. Microsc., Part 2* **1994**, *174*, 69-73.
(42) Popovic, Z. D.; Loutfy, R. O.; Hor, A.-M. *Can, J. Chem.* **1985**, *63*, 134-139.
(43) Higgins, D. A.; Hall, J. E.; Xie, A. *Acc. Chem. Res.* **2005**, *38*, 137-145.

Self-Assembled Photoactive Polyelectrolyte/ Perylene-Diimide Composites

Aifang Xie, Bei Liu, Jeffrey E. Hall, Sarah L. Barron, and Daniel A. Higgins*

Department of Chemistry, Kansas State University, Manhattan, Kansas 66506

Received November 17, 2004. In Final Form: February 1, 2005

A new class of polyelectrolyte-surfactant (PE-surf) composites having potential applications as thin film organic semiconductors is introduced. These materials are comprised of cationic asymmetrically substituted perylene diimides and oppositely charged poly(acrylate) polyanions. Thin films of the composite materials are prepared by mixing and drop casting aqueous solutions of the two precursors onto appropriate substrates. The resulting materials yield photovoltages of >140 mV for ≈0.6 W/cm^2 illumination intensities, when incorporated in p−n heterojunction devices. Solution-phase spectra obtained from the PE-surf complexes exhibit excimer-like emission and evidence for formation of weakly coupled aggregates in the ground state. Wide-angle X-ray scattering data show the composite films are locally amorphous, while small-angle X-ray data are consistent with a mixture of polymorphic structures that incorporate planar PE-surf bilayers of 3.9-nm repeat distances. Images obtained by conventional far-field light microscopy and multiphoton-excited fluorescence microscopy (MPEFM) indicate that the films are heterogeneous, incorporating submicrometer sized clusters dispersed among much thinner film regions that also incorporate dye. Polarization-dependent MPEFM studies prove the clusters are semiorganized, yielding order parameters (s and P_4) of 0.09 and 0.01 for in-plane alignment of the chromophores, consistent with a relatively high degree of disorder.

Introduction

Perylene diimides are important molecular building blocks that are currently being investigated for use in a variety of photoactive organic materials.[1−3] They have been used previously as the electron-transporting (or n-type) medium in organic heterojunction photovoltaics.[2] At present, few alternative n-type organic semiconductors exist. Molecules containing a perylene diimide core have also been proposed for use in artificial photosynthesis,[4,5] while related compounds (i.e., the naphthalene diimides) have been investigated as photoactive DNA intercalators for photodynamic cancer therapies.[6,7] The broad utility of these materials arises in part from the ease by which the perylene diimide core can be chemically, photochemically, or electrochemically reduced (they can also be oxidized).[8−10]

Another important attribute that has led to widespread use of the perylene diimides is the relative ease by which compounds having different chemical and physical properties can be synthesized. Perylene diimides in general are prepared by reacting perylene tetracarboxylic dianhydride with appropriate amines. A range of chemically distinct species can easily be prepared by simply using different precursor amines. Most commonly, the materials prepared are symmetrically substituted. Previously prepared perylene diimides include crystalline materials,[11,12] as well as thermotropic[3,13] and lyotropic liquid crystals.[14,15] The primary goal in many of these studies was to develop photoactive materials that self-assemble into organized phases.

Organized perylene diimide thin films have been prepared previously by vapor deposition,[12] spin casting,[3] self-assembly via hydrogen bonding,[16,17] and Langmuir−Blodgett techniques.[18] In many situations, the molecules employed formed solid crystalline or microcrystalline materials (at least at room temperature).[3] X-ray diffraction[13] and optical microscopy[19,20] studies showed in many instances the presence of organized materials having a high degree of order over a wide range of distance scales (i.e., from angstroms to micrometers).

In this publication, we introduce a new class of self-assembled polyelectrolyte/perylene-diimide composites that exhibit many unique physical and organizational attributes, making them potentially useful as alternatives to existing small-molecule and conjugated-polymer-based organic semiconductors. For the preparation of these materials, a new type of amphiphilic perylene diimide has been synthesized. This molecule incorporates a cationic functional group on one end and a hydrophobic

* Author to whom correspondence should be addressed. E-mail: higgins@ksu.edu.

(1) Law, K.-Y. *Chem. Rev.* **1993**, *93*, 449.
(2) Gregg, B. A. *J. Phys. Chem. B* **2003**, *107*, 4688.
(3) Cormier, R. A.; Gregg, B. A. *Chem. Mater.* **1998**, *10*, 1309.
(4) Giaimo, J. M.; Gusev, A. V.; Wasielewski, M. R. *J. Am. Chem. Soc.* **2002**, *124*, 8530.
(5) Lukas, A. S.; Zhao, Y.; Miller, S. E.; Wasielewski, M. R. *J. Phys. Chem. B* **2002**, *106*, 1299.
(6) Rogers, J. E.; Weiss, S. J.; Kelly, L. A. *J. Am. Chem. Soc.* **2000**, *122*, 427.
(7) Yen, S.-F.; Gabbay, E. J.; Wilson, W. D. *Biochemistry* **1982**, *21*, 2070.
(8) Zhao, Y.; Wasielewski, M. R. *Tetrahedron Lett.* **1999**, *40*, 7047.
(9) Williams, M. E.; Murray, R. W. *Chem. Mater.* **1998**, *10*, 3603.
(10) Lee, S. K.; Zu, Y.; Herrmann, A.; Geerts, Y.; Müllen, K.; Bard, A. J. *J. Am. Chem. Soc.* **1999**, *121*, 3513.
(11) Iverson, I. K.; Casey, S. M.; Seo, W.; Tam-Chang, S.-W. *Langmuir* **2002**, *18*, 3510.
(12) Klebe, G.; Graser, F.; Hädicke, E.; Berndt, J. *Acta Crystallogr.* **1989**, *B45*, 69.
(13) Schlettwein, D.; Back, A.; Schilling, B.; Fritz, T.; Armstrong, N. R. *Chem. Mater.* **1998**, *10*, 601.
(14) Liu, S.-G.; Sui, G.; Cormier, R. A.; Leblanc, R. M.; Gregg, B. A. *J. Phys. Chem. B* **2002**, *106*, 1307.
(15) Iverson, I. K.; Tam-Chang, S.-W. *J. Am. Chem. Soc.* **1999**, *121*, 5801.
(16) Schenning, A. P. H. J.; Herrikhuyzen, J. V.; Jonkheijm, P.; Chen, Z.; Würthner, F.; Meijer, E. W. *J. Am. Chem. Soc.* **2002**, *124*, 10252.
(17) Würthner, F.; Thalacker, C.; Sautter, A. *Adv. Mater.* **1999**, *11*, 754.
(18) Antunes, P. A.; Constantino, C. J. L.; Aroca, R. F.; Duff, J. *Langmuir* **2001**, *17*, 2958.
(19) Conboy, J. C.; Olson, E. J. C.; Adams, D. M.; Kerimo, J.; Zaban, A.; Gregg, B. A.; Barbara, P. F. *J. Phys. Chem. B* **1998**, *102*, 4516.
(20) Adams, D. M.; Kerimo, J.; Olson, E. J. C.; Zaban, A.; Gregg, B. A.; Barbara, P. F. *J. Am. Chem. Soc.* **1997**, *119*, 10608.

10.1021/la0471700 CCC: $30.25
Published on Web 03/29/2005

alkane chain on the opposite end. It mimics more conventional lyotropic liquid crystals (i.e., surfactants) and exhibits water solubility to the hundred μM level. When aqueous solutions of this compound are combined with solutions of oppositely charged (i.e., anionic) polyelectrolytes, photoactive polyelectrolyte-surfactant (PE-surf)[21-23] composites are obtained.[24-26] Like existing PE-surf composites, the present materials self-assemble via a highly cooperative mechanism involving electrostatic interactions between the polyelectrolyte and the perylene diimide molecules and hydrophobic interactions between their alkane tails. Unlike more common PE-surfs, these materials also utilize π-stacking interactions as an additional means for driving self-assembly. The final PE-surf composites are believed to consist of nonpolar regions (i.e., comprised of the aromatic ring structures and hydrocarbon tails of the perylene diimides) sandwiched between ionic layers incorporating the charged diimide headgroups and the oppositely charged polyelectrolyte.

When stoichiometric (or nearly stoichiometric) PE-surfs are formed from perylene diimide and polyelectrolyte solutions, the complexes become water-insoluble and precipitate. Nonstoichiometric composites, however, remain water-soluble and can be spin cast, drop cast, or spray cast as thin films onto a variety of substrates. These water-soluble composites show clear spectroscopic evidence for aggregation of the perylene diimides, indicating they are closely associated, even at very low stoichiometric loadings. Physical film morphology and dye organization are characterized here using X-ray scattering, conventional far-field optical microscopy, and polarization-dependent multiphoton-excited fluorescence microscopy (MPEFM).[27-29] The X-ray data point to the presence of nanometer-scale organization in the films, while the MPEFM data are used to probe chromophore order in submicrometer sized domains found in the films.

Experimental Section

Synthesis of *N*-(Dodecyl)-*N*′-(2-(*N*,*N*-dimethylamino)-ethyl)perylene-3,4,9,10-tetracarboxylic Diimide (C_{12}-PDI). Perylene-3,4,9,10-tetracarboxylic dianhydride, *n*-dodecylamine, and *N*,*N*-dimethylethylenediamine were all obtained from Aldrich and were used as received. A single-pot procedure was employed in this synthesis.

To a 250-mL round-bottom flask was added 214 mg (0.545 mmol) of the dianhydride, 111 mg (0.599 mmol) dodecylamine, and 150 mL of pyridine. In a separate vial, 55 mg (0.62 mmol) of *N*,*N*-dimethylethylenediamine was dissolved in a few mLs of pyridine. One-third of this solution was immediately transferred to the round-bottom flask, which was subsequently fitted to a reflux condenser and a nitrogen purge line. The mixture was refluxed with vigorous stirring for approximately 24 h. The remaining dimethylethylenediamine solution was added in two portions during the initial 8–10 h. The pyridine was subsequently removed using a rotary evaporator. The resulting crude reaction mixture contained two symmetrically substituted perylene diimides (i.e., substituted with dodecylamine and dimethylethylenediamine), along with the desired asymmetrically substituted compound (C_{12}-PDI). The asymmetric compound was obtained in high purity and in 21% yield as the intermediate band in column chromatography using 20:1 chloroform:ethanol as the mobile phase and a silica gel column. ^{1}H NMR δ_H (400 MHz, $CDCl_3$): 0.88 (t, 3H, $NC_{11}H_{22}CH_3$), 1.26 (m, 18H, $NCH_2CH_2C_9H_{18}CH_3$), 1.77 (m, 2H, $NCH_2CH_2C_{10}H_{21}$), 2.39 (s, 6H, $NCH_2CH_2N(CH_3)_2$), 2.71 (t, 2H, $NCH_2CH_2N(CH_3)_2$), 4.20 (t, 2H, $NCH_2C_{11}H_{23}$), 4.37 (t, 2H, $NCH_2CH_2N(CH_3)_2$, 8.6 (m, 8H, perylene).

Synthesis of *N*-(Dodecyl)-*N*′-(2-(trimethylammonio)-ethyl)perylene-3,4,9,10-tetracarboxylic Diimide Iodide (C_{12}-PDI$^+$·I$^-$), MW = 771.8 g/mol. To a 50-mL round-bottom flask containing a stir bar and 25 mL of chloroform was added 63 mg (0.10 mmol) of C_{12}-PDI and 70 mL (1.1 mmol) of iodomethane. The reaction mixture was refluxed overnight under a nitrogen atmosphere. C_{12}-PDI$^+$·I$^-$ precipitated from solution as the reaction proceeded. The final product was collected in 77% yield by either vacuum filtration or centrifugation from a chloroform suspension.

Preparation of C_{12}-PDI$^+$–Polyelectrolyte Composites. Aqueous solutions of C_{12}-PDI$^+$·I$^-$ having concentrations of ≈130 μM were prepared by first dissolving the compound in ≈25 mL of spectrophotometric grade methanol. Another 25 mL of high-purity water was added, and the solution was brought to a boil, with stirring. Once the solution volume reached ≈15 mL, it was transferred to a 25-mL volumetric flask, allowed to cool, and diluted to the mark with high-purity (18 MΩcm) water. Sodium poly(acrylate) (NaPA, 5100 M_w) was obtained from Aldrich and was used as received. Aqueous solutions of PA$^-$ were prepared using high-purity water. C_{12}-PDI$^+$/PA$^-$ composites were obtained in a range of stoichiometric loadings for bulk solution-phase experiments by simply mixing appropriate volumes of the aqueous C_{12}-PDI$^+$·I$^-$ and PA$^-$ solutions.

Samples employed for optical microscopic imaging were prepared as follows. Approximately 10 mL of ≈106 μM PA$^-$ (monomer concentration) solution was transferred to a beaker and heated, with stirring, to ≈60 °C using a water bath. The C_{12}-PDI$^+$·I$^-$ solution (≈130 μM) was then added in a single 3–5 mL aliquot. This mixture was then concentrated by a factor of 3–5 with continued heating and stirring. Thin films were prepared by drop casting the hot solution onto a microscope cover glass. Finally, the resulting films were dried in an oven at temperatures up to ≈90 °C. Film thickness in these materials was determined by atomic force microscopy to be 200 nm in central film regions, where most subsequent measurements were made. Thin films for characterization by X-ray methods were prepared in a similar fashion (at the same stoichiometric loadings), except that thicker films were prepared by drop casting the solution several times onto the same glass slide.

Multiphoton-Excited Fluorescence Microscopy (MPEFM). Fluorescence images of the C_{12}-PDI$^+$/PA$^-$ thin films were recorded on a sample scanning confocal microscope. This microscope has been described previously.[30,31] Briefly, it is constructed upon an inverted light microscope (Nikon TE-300) and employs a "closed-loop" sample scanning stage (Queensgate NPS-XY-100A) for sample positioning and image acquisition. The 850-nm output of a mode-locked Ti:sapphire laser (Coherent Mira-900, 170 fs pulse width, 76 MHz repetition rate) was used as the excitation source. Light from the laser was directed through polarization optics to control the power and the incident polarization state, prior to directing it into the microscope by reflection from a harmonic beam splitter (CVI). A broad-band half-wave plate (Special Optics, 700–900 nm functional range) was employed to set the incident polarization state. The excitation light was focused to a diffraction-limited spot in the sample using a 100×, 1.3 numerical aperture (NA) oil-immersion objective. The average incident power employed was always maintained below 1 mW. Excitation of C_{12}-PDI$^+$ fluorescence in this system occurs by two-photon absorption (see below). The same objective was used to collect the fluorescence subsequently emitted by the sample. The collected light passed back through the half-wave plate and harmonic beam splitter and was subsequently directed through two 700-nm short-pass filters and onto the photosensitive surface of either a single-photon-counting PMT (Hamamatsu

(21) Antonietti, M.; Conrad, J.; Thünemann, A. *Macromolecules* **1994**, *27*, 6007.
(22) MacKnight, W. J.; Ponomarenko, E. A.; Tirrell, D. A. *Acc. Chem. Res.* **1998**, *31*, 781.
(23) Zhou, S.; Chu, B. *Adv. Mater.* **2000**, *12*, 545.
(24) Chen, L.; Xu, S.; McBranch, D.; Whitten, D. *J. Am. Chem. Soc.* **2000**, *122*, 9302.
(25) Thünemann, A. F.; Ruppelt, D. *Langmuir* **2000**, *16*, 3221.
(26) Thünemann, A. F.; Ruppelt, D. *Langmuir* **2001**, *17*, 5098.
(27) Denk, W.; Strickler, J. H.; Webb, W. W. *Science* **1990**, *248*, 73.
(28) Gratton, E.; Barry, N. P.; Beretta, S.; Celli, A. *Methods* **2001**, *00*, 103.
(29) Bhawalkar, J. D.; He, G. S.; Prasad, P. N. *Rep. Prog. Phys.* **1996**, *59*, 1041.
(30) Springer, G. H.; Higgins, D. A. *Chem. Mater.* **2000**, *12*, 1372.
(31) Luther, B. J.; Springer, G. H.; Higgins, D. A. *Chem. Mater.* **2001**, *13*, 2281.

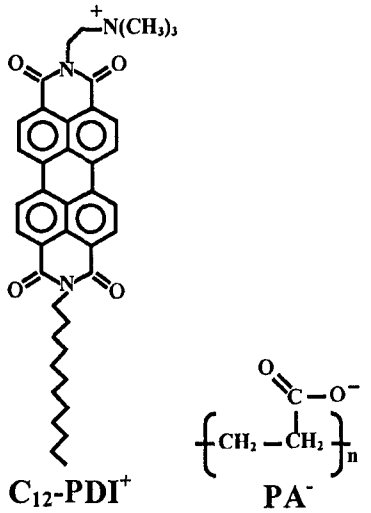

Figure 1. Chemical structures of C_{12}-PDI$^+$ and PA$^-$.

HC135−01) or a single-photon-counting avalanche diode (Perkin-Elmer, SPCM-AQ141). Images were recorded in raster-scanning mode, using LabView software written in house. Polarization-dependent fluorescence excitation experiments were performed using an "angle-encoded" motorized rotation stage (New Focus) with the broad-band half-wave plate.

Bulk Sample Characterization. Solution-phase fluorescence spectra of C_{12}-PDI$^+$·I$^-$ and the C_{12}-PDI$^+$/PA$^-$ complexes were obtained using a commercial spectrofluorimeter (SPEX Fluoromax) and conventional one-photon excitation. UV−vis absorption spectra were recorded on a diode array spectrometer (HP 8453).

X-ray scattering data from the thin films were obtained using a Bruker D8 Advance instrument. This system employs Cu Kα radiation ($\lambda = 1.54$ angstroms) with an applied voltage of 40 kV and a current of 40 mA. Characteristic spacings, d, associated with the organized film structures were determined from their X-ray scattering angles 2θ as follows:

$$d = \frac{\lambda}{2 \sin \theta} \tag{1}$$

Results and Discussion

The chemical structures of C_{12}-PDI$^+$ and PA$^-$ are shown in Figure 1. C_{12}-PDI$^+$ is related to several previously studied perylene diimides.[3,13−15] Since it incorporates the same aromatic core, it is expected to exhibit similar photophysical and electrochemical properties. Because it incorporates a cationic headgroup, it is also modestly water-soluble. Water-soluble, symmetrically substituted ionic perylene diimides have been described previously and are known to behave as lyotropic liquid crystals.[14,15] C_{12}-PDI$^+$ differs from these in that it is structurally more similar to conventional amphiphilic surfactants. The C_{12}-PDI$^+$ species indeed exhibits modest surface activity in aqueous solutions, depressing the measured surface tension of the air−water interface from 71.0 mN/m to 65.4 mN/m at a concentration of 100 μM, as determined by the capillary rise method.

C_{12}-PDI$^+$/PA$^-$ complexes are readily prepared by simply mixing aqueous solutions of C_{12}-PDI$^+$ and PA$^-$. In solutions where the concentration of C_{12}-PDI$^+$ approaches that of the PA$^-$ monomer, water-insoluble (nearly) stoichiometric complexes form that rapidly precipitate from solution. Nonstoichiometric complexes (i.e., 50% or lower PA$^-$ monomer loadings), however, remain soluble in the absence of other ionic species. These systems represent a new class of PE-surf composite and are expected to show some of the same chemical and physical properties exhibited by more common PE-surfs.[21−23] Specifically, the composites should possess mechanical and film-forming properties that differ substantially from films of pure perylene diimides, because of the presence of the polyelectrolyte. Importantly, thin films of these composites should also exhibit the same technologically useful photoactivity (i.e., yielding a photovoltage and photocurrent under illumination) as films of pure perylene diimides.

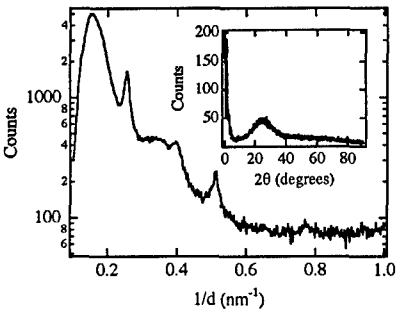

Figure 2. Representative SAXS data for films prepared from C_{12}-PDI$^+$/PA$^-$ complexes. All films were prepared by drop casting aqueous solutions of the C_{12}-PDI$^+$/PA$^-$ complexes on microscope cover glasses. This particular film was dried at ≈90 °C prior to characterization. The inset shows WAXS data, which is indicative of significant disorder on angstrom length scales. The x-axis in the SAXS data has been corrected for an ≈0.25° error in 2θ.

The possible utility of the C_{12}-PDI$^+$/PA$^-$ composites as alternative organic semiconducting/photovoltaic materials was assessed by preparing and testing simple p−n heterojunction devices. These materials consisted of two indium tin oxide coated glass slides onto which thin films of the C_{12}-PDI$^+$/PA$^-$ composite (serving as the electron-transporting or n-type material) and TPD (a well-known hole-transporting or p-type organic semiconductor)[1] were cast and dried. Each of these films was ≈2-μm thick. The cell was then assembled and cemented together. Under illumination with 488-nm light (≈0.6 W/cm^2), these rudimentary devices exhibited photovoltages of > 140 mV. The semiconducting properties of these materials will be explored in more detail in future publications.

X-ray Structural Information. PE-surf systems based on more conventional surfactants and similar polyelectrolytes exhibit a diversity of morphological structures, showing organization on relatively large (i.e., a few nanometers) length scales.[21,22] Generally, they exhibit little short-range (angstrom scale) organization. PE-surfs have previously been observed to form planar bilayers,[32−34] perforated or undulating bilayers,[21,32] cubic structures,[32,35] and hexagonal phases.[25,36] On the basis of these previous studies, and the planar nature of the perylene chromophore, it is hypothesized that thin films formed from C_{12}-PDI$^+$/PA$^-$ composites should incorporate planar bilayers. The perylene diimides are expected to form "π-stacks" within the bilayers.

X-ray scattering data obtained in studies of the C_{12}-PDI$^+$/PA$^-$ composite thin films are shown in Figure 2. The data were collected in both wide-angle (WAXS) and small-angle (SAXS) geometries. The WAXS data in all C_{12}-PDI$^+$/PA$^-$ films exhibit a weak, broad peak in the 2θ

(32) Antonietti, M.; Burger, C.; Effing, J. *Adv. Mater.* **1995**, *7*, 751.
(33) Wenzel, A.; Antonietti, M. *Adv. Mater.* **1997**, *9*, 487.
(34) Ponomarenko, E. A.; Waddon, A. J.; Tirrell, D. A.; MacKnight, W. J. *Langmuir* **1996**, *12*, 2169.
(35) Antonietti, M.; Conrad, J. *Angew. Chem., Int. Ed. Engl.* **1994**, *33*, 1869.
(36) Zhou, S.; Yeh, F.; Burger, C.; Chu, B. *J. Phys. Chem. B* **1999**, *103*, 2107.

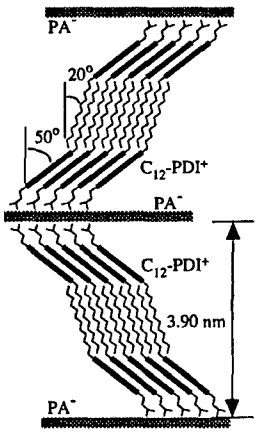

Figure 3. Proposed structure of the bilayers present in the C_{12}-PDI$^+$/PA$^-$ composite thin films. The interdigitated alkane chains are tilted by ≈20° from the bilayer normal and the perylene chromophores are tilted by ≈50°. The perylene chromophores are viewed "edge-on".

= 15−35° range. WAXS data obtained from films of pure C_{12}-PDI$^+$ or pure PA$^-$ exhibit this same feature. Its appearance indicates the materials are disordered on short (i.e., 0.25−0.60 nm) length scales. As a result, it may be concluded that neither the alkane chains of the C_{12}-PDI$^+$ molecules nor the polymer hydrocarbon backbones are ordered to any significant degree. It may also be concluded that the perylene chromophores, which often exhibit relatively strong π-stacking interactions in crystalline materials, are relatively disordered.

In contrast to the WAXS data, the SAXS data indicate the presence of long-range (occurring over several nanometers) organization in the C_{12}-PDI$^+$/PA$^-$ composites. Most noteworthy is the appearance of a series of relatively sharp diffraction peaks corresponding to multiple (up to three) orders of diffraction from a single film structural feature. Here, these diffraction peaks are attributed to the bilayers believed to be present. Figure 3 shows the proposed model for C_{12}-PDI$^+$/PA$^-$ composite organization. From the SAXS data, the bilayer spacing in the films is deduced to be 3.9 nm. The relatively small bilayer spacing (C_{12}-PDI$^+$ is calculated to be ≈3 nm in length, assuming an extended alkane chain) is most likely due to "tilting" of the C_{12}-PDI$^+$ species, accompanied by significant interdigitation of the alkane chains. Assuming extended chains and full interdigitation, the alkane chains are still required to be tilted by ≈20° to form bilayers with 3.9-nm spacings. In such a structure, the C_{12}-PDI$^+$ chromophores are also tilted by ≈50°. Tilting of the chromophores leads to an offset in the π-stacking of the chromophores and a shift in the electronic transition energies within the aggregate.[11]

While the narrow peaks observed in the SAXS data are consistent with bilayer structures, the broader peaks also observed (see Figure 2) indicate that the film organization is actually more complicated. Upon initial inspection, the data appear similar to those reported previously for PE-surfs exhibiting structures of cubic symmetry.[35,37] The formation of such structures is believed unlikely in the present samples because of the influence of the large, planar perylene diimide chromophores. It is unlikely such molecules would form spheroidal micelles or the undulating cubic phases proposed previously.[35,37] Therefore, the series of broad peaks likely results from other types of

(37) Antonietti, M.; Burger, C.; Conrad, J.; Kaul, A. *Macromol. Symp.* **1996**, *106*, 1.

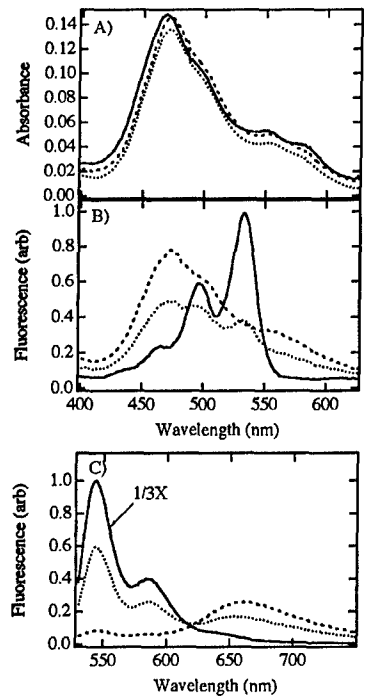

Figure 4. (A) Absorption, (B) fluorescence excitation, and (C) emission spectra for C_{12}-PDI$^+$I$^-$ and C_{12}-PDI$^+$/PA$^-$ complexes in aqueous solution. The composite spectra are reported for a series of C_{12}-PDI$^+$/PA$^-$ stoichiometries. The concentration of C_{12}-PDI$^+$ was maintained at 10 μM in all cases. The PA$^-$ (monomer) concentration was 0.0 μM (solid line, PDI$^+$I$^-$), 15 μM (dotted line), and 30 μM (dashed line) in these samples. The emission and excitation wavelengths in the excitation and emission spectra were 650 and 488 nm, respectively.

organized structures also present in the films. The C_{12}-PDI$^+$/PA$^-$ composites may simultaneously form two or more different polymorphs, or there may be two or more chemically distinct forms of the composite present that self-assemble in different ways. In fact, SAXS studies of pure C_{12}-PDI$^+$ films exhibit diffraction patterns very similar to the series of broad peaks depicted in Figure 2. Hence, the broad peaks are tentatively assigned to C_{12}-PDI$^+$ phases that do not incorporate polyelectrolyte. These "pure" C_{12}-PDI$^+$ structures are clearly more disordered and less tightly packed than the relatively well-ordered composite bilayers. Their greater spacing could result from less efficient packing of the molecules brought about by enhanced electrostatic repulsion of the ionic C_{12}-PDI$^+$ headgroups. Unfortunately, it is not possible to determine the actual film structures in greater detail at the present time. Future studies employing C_{12}-PDI$^+$ and related compounds incorporating alkane groups of different lengths will be used to further address this issue. Annealing methods will also be used to change/control the organization; the results will provide a more concrete picture of the organization.

Bulk Spectroscopic Data. While the X-ray data described above indicate a lack of short-range order in the C_{12}-PDI$^+$/PA$^-$ composites, absorption and fluorescence spectra of the composites indicate that the chromophores are indeed aggregated, and hence, positioned in close proximity to each other. Figure 4 depicts the solution-phase UV−vis absorption, fluorescence excitation, and fluorescence emission spectra obtained from a series of composites. These composites were prepared with varying polyelectrolyte concentrations to yield a series of complexes having different stoichiometries. NaCl was added to the

solutions as necessary, to maintain an approximately constant ionic strength.

The absorption spectra obtained from aqueous C_{12}-PDI$^+$·I$^-$ solutions (i.e., in the absence of polyelectrolyte) provide important evidence for partial aggregation (or dimerization) of the chromophores, even at concentrations as low as 10 μM (see Figure 4). These spectra are broadened and blue-shifted from those observed for the monomeric species in dilute solutions of polar organic solvents such as ethanol (not shown). In contrast, the fluorescence excitation and emission spectra of these same solutions are nearly identical to those of the monomeric species dissolved in organic solvents. The intensity of fluorescence from the aqueous solutions, however, is greatly decreased. For example, the emission yield of C_{12}-PDI$^+$ is measured to be 0.73 in ethanol (using rhodamine 6G as a standard), while that measured in aqueous solution (assuming C_{12}-PDI$^+$ is present in its monomeric form) would be <0.01.

From these studies, as well as those performed on related compounds, it is concluded that the C_{12}-PDI$^+$·I$^-$ is almost completely aggregated at 10 μM concentrations in aqueous solution. The fluorescence excitation and emission spectra then reflect the presence of a small amount of residual monomeric C_{12}-PDI$^+$. The aggregates formed (absent PA$^-$) appear to be nonfluorescent.

Upon addition of an excess of PA$^-$, the emission spectrum shifts dramatically to the red (from 544 to 660 nm) and broadens significantly. The emission yield also drops precipitously, but the species formed remain slightly fluorescent. Broadened, red-shifted emission like that exhibited by the C_{12}-PDI$^+$/PA$^-$ composite is usually attributed to the formation of excimers.[9,38,39] Excimer formation is also supported by the absence of new red-shifted peaks in the absorption and fluorescence excitation spectra of the composite. However, the blue-shifted absorption and excitation spectra that are observed suggest the C_{12}-PDI$^+$/PA$^-$ complex is also aggregated in the ground state (similarly to C_{12}-PDI$^+$ alone). Ground-state aggregates have also been observed in related (but covalently linked) perylene diimides, on the basis of NMR studies.[38] In the present materials, it is concluded that aggregation of the chromophores (in the ground state) in the presence of PA$^-$ facilitates excimer formation by positioning the chromophores in closer proximity to each other. The fact that excimer emission is not observed from the aqueous C_{12}-PDI$^+$ solutions absent PA$^-$ indicates the polyelectrolyte plays an important role in controlling aggregate structure, possibly by shielding the positive charges on the C_{12}-PDI$^+$ molecules from each other. Studies in which a polycation was used in place of PA$^-$ showed no evidence of excimer emission, proving that these effects are a direct result of ionic interactions between C_{12}-PDI$^+$ and PA$^-$. Overall, the spectra observed for the C_{12}-PDI$^+$/PA$^-$ composites are similar to those obtained previously for other liquid crystalline perylene diimides.[13] On the basis of this prior work, and the results presented here, it may then be concluded that the chromophores form weakly interacting π-stacks in the ground state and much more strongly interacting ones upon excitation.

Optical Microscopy Studies. Conventional far-field optical microscopy and multiphoton-excited fluorescence microscopy (MPEFM)[27-29] studies provide information on film quality and overall film morphology, as well as valuable data on chromophore organization on submicrometer length scales. Figure 5 shows an optical micrograph of a C_{12}-PDI$^+$/PA$^-$ composite film recorded on a conventional transmission microscope. The film is clearly inhomogeneous, exhibiting structures having a broad range of sizes from several micrometers (lateral size) down to the smallest resolvable features (i.e., of diffraction-limited size). On the whole, such films appear red/brown throughout, a good indication that C_{12}-PDI$^+$ is well dispersed in the films. As will be described in forthcoming publications, the film morphology depends not only upon C_{12}-PDI$^+$/PA$^-$ stoichiometry but also on film treatment conditions (e.g., annealing).

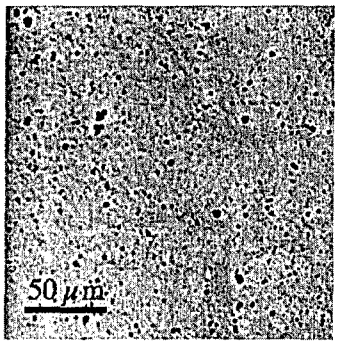

Figure 5. Large area optical micrograph of a C_{12}-PDI$^+$/PA$^-$ composite thin film on a microscope cover glass.

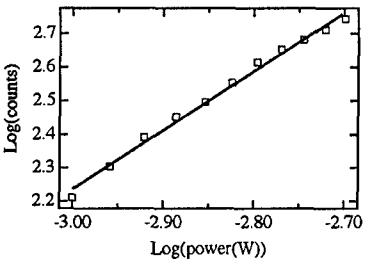

Figure 6. Power dependence of multiphoton fluorescence excitation in the C_{12}-PDI$^+$/PA$^-$ thin films. Also shown is the straight-line fit to these data, which yields a slope of ≈2, indicative of a two-photon excitation process.

Compared to conventional far-field methods, MPEFM provides improved image contrast and better spatial resolution.[27,28,40] Because of the nonlinear nature of fluorescence excitation in MPEFM, the samples can be imaged with resolution beyond the conventional diffraction limit.[40] The lateral spatial resolution in MPEFM is approximately given by $0.61\lambda/(\mathrm{NA}\sqrt{n})$, where n is the number of photons participating in the excitation process. Figure 6 plots the power dependence of fluorescence excitation in the C_{12}-PDI$^+$/PA$^-$ composite thin films. A least-squares fit of these data yields a line of slope ≈2, indicating that fluorescence excitation is dominated by two-photon absorption. Under the present experimental conditions (850-nm incident light, NA = 1.3, n = 2), a resolution of ≈280 nm is predicted. Background signals are also greatly reduced in MPEFM because fluorescence excitation only occurs in the focal volume of the microscope objective. The background-free imaging capability of MPEFM is an important advantage when very weakly fluorescent materials such as the C_{12}-PDI$^+$/PA$^-$ composites are to be imaged. Finally, multiphoton excitation processes are also strongly polarization dependent, providing the greatest sensitivity in detailed studies of local chromophore organization.[41]

(38) Wang, W.; Han, J. J.; Wang, L.-Q.; Li, L.-S.; Shaw, W. J.; Li, A. D. Q. *Nano Lett.* **2003**, *4*, 455.
(39) Ford, W. E.; Kamat, P. V. *J. Phys. Chem.* **1987**, *91*, 6373.
(40) Deitche, J.; Kempe, M.; Rudolph, W. *J. Microsc., Part 2* **1994**, *174*, 69.
(41) Higgins, D. A.; Luther, B. J. *J. Chem. Phys.* **2003**, *119*, 3935.

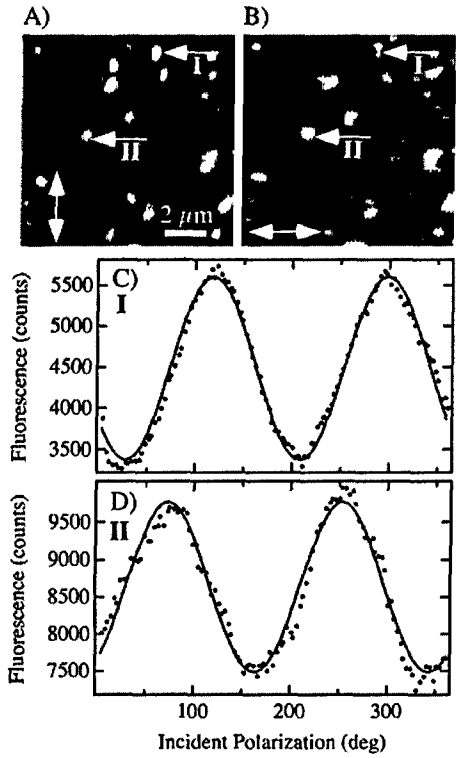

Figure 7. (A) and (B) MPEFM fluorescence images recorded using the two different excitation polarizations shown for C_{12}-PDI$^+$/PA$^-$ thin films. These data depict the strong polarization dependence of multiphoton fluorescence excitation in some domains of these materials. (C) and (D) Polarization dependence of multiphoton fluorescence excitation for the specific C_{12}-PDI$^+$/PA$^-$ domains (I and II, respectively) indicated by the arrows on the images. A small background signal was subtracted from the data.

The lowest energy electronic transition in perylene diimides similar to C_{12}-PDI$^+$ is polarized along the long axis of the chromophore.[42-44] While there are nearby transitions that are short-axis polarized, they are extremely weak. In addition, if D_{2h} symmetry is assumed for the chromophore, the main long-axis transition is two-photon forbidden for short-axis polarized photons. These factors ensure that the transition excited in MPEFM imaging is the long-axis polarized transition of the C_{12}-PDI$^+$ chromophore. Hence, any polarization dependence observed by two-photon fluorescence excitation indicates the direction of long-axis orientation.

Figure 7 depicts representative MPEFM images of the C_{12}-PDI$^+$/PA$^-$ composite thin films. As is readily apparent in these images, the films are comprised of small fluorescent domains surrounded by darker (i.e., more weakly fluorescent) regions. Much of this variability is due to variations in the amount of C_{12}-PDI$^+$ present. The fluorescent domains clearly contain significant concentrations of C_{12}-PDI$^+$. Fluorescence spectra recorded from the bright regions are similar to (albeit broader than) those obtained from the composites in aqueous solution by one-photon excitation (see Figure 4). These observations prove that emission from the film arises primarily from excitation of aggregates. Little information on the extent to which C_{12}-PDI$^+$ is incorporated in the dark regions can be obtained, however, because of the strong orientation/polarization dependence of multiphoton excitation. C_{12}-PDI$^+$ chromophores oriented with their long axes perpendicular to the film plane are not efficiently excited, and hence such regions appear dark in the MPEFM images. The darker regions may also incorporate non-fluorescent C_{12}-PDI$^+$ aggregates formed without complexation to PA$^-$. The presence of such species was proposed above as an explanation for the complicated SAXS results obtained from these films.

The appearance of small, often diffraction-limited features in these images suggests that any bilayer structures formed are limited in their spatial extent (i.e., to lateral dimensions of <1 μm). In this instance, small domains containing bilayers such as those in Figure 3 could orient in almost any direction. Such disorder is consistent with the data reported herein.

The images shown in Figure 7A and B were recorded using orthogonal excitation polarizations. They show modest polarization-dependent changes in the fluorescence excitation efficiency from the bright features. Two sample features exhibiting this behavior are highlighted (see arrows I and II) in the images. These results prove that the C_{12}-PDI$^+$ chromophores present in the fluorescent domains are organized. They also indicate that the long molecular axes of the C_{12}-PDI$^+$ chromophores in these regions are tilted off the sample normal (i.e., they have a component parallel to the film plane). Again, in the model presented in Figure 3, the chromophores are tilted by 50° from the bilayer (and sample) normal. Bilayers oriented parallel to the substrate surface should then yield significant fluorescence.

Single-point polarization dependent studies of the fluorescent domains have been performed to better understand chromophore order in the composites. Figure 7C and D depicts representative examples of these data, recorded for points I and II, respectively, shown in Figure 7A and B. The polarization-dependent fluorescence data can be fit to a model for the nonlinear optical response of the materials to obtain a measure of the local order parameters for in-plane C_{12}-PDI$^+$ chromophore organization.

The total (unpolarized) fluorescence, I_{fl}, from the sample excited by two identical, polarized incident photons, $\mathbf{E}(\omega)$, can be described by the following expression:

$$I_{fl} \propto |\mathbf{T}^{agg}(2\omega):\mathbf{E}(\omega)\mathbf{E}(\omega)|^2 {I_{inc}}^2 \qquad (2)$$

where $\mathbf{T}^{agg}(2\omega)$ is the second-rank tensor denoting the nonlinear susceptibility of the C_{12}-PDI$^+$/PA$^-$ composite excited at twice the frequency of the incident light. The elements of the nonlinear susceptibility tensor for the aggregate, $\mathbf{T}_{IJ}^{agg}$, can then be related to those of the molecular susceptibility tensor, $\mathbf{T}_{ij}^{mol}$, via a simple coordinate transformation:

$$\mathbf{T}_{IJ}^{agg} = \sum_{i,j} \langle R_{Ii} R_{Jj} \rangle \mathbf{T}_{ij}^{mol} \qquad (3)$$

where R_{Ii} and R_{Jj} represent direction cosines taken between the molecular and aggregate Cartesian coordinate systems. Figure 8 depicts the molecular and aggregate coordinate systems, including the two relevant angles associated with the coordinate transformation, θ and ϕ. As shown in Figure 8, the molecular z-axis is defined as the long axis of the C_{12}-PDI$^+$ chromophore. The Z-axis of

(42) Kazmaier, P. M.; Hoffmann, R. *J. Am. Chem. Soc.* **1994**, *116*, 9684.
(43) Adachi, M.; Murata, Y.; Nakamura, S. *J. Phys. Chem.* **1995**, *99*, 14240.
(44) Struijk, C. W.; Sieval, A. B.; Dakhorst, J. E. J.; van Dijk, M.; Kimkes, P.; Koehorst, R. B. M.; Donker, H.; Schaafsma, T. J.; Picken, S. J.; van de Craats, A. M.; Warman, J. M.; Zuilhof, H.; Sudhölter, E. J. R. *J. Am. Chem. Soc.* **2000**, *122*, 11057.

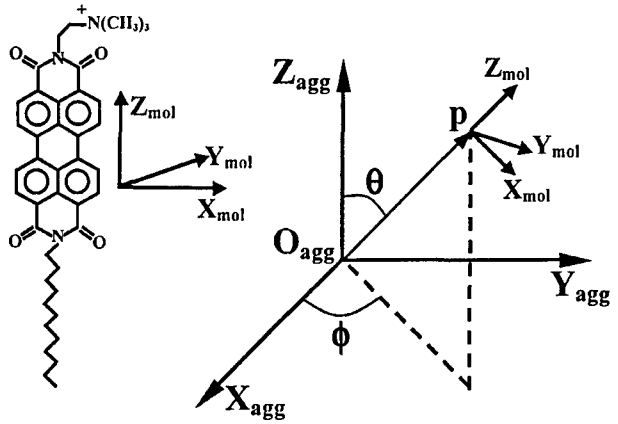

Figure 8. Molecular and aggregate coordinate systems and the relevant angles relating the two. The molecule is positioned at point p, with the coordinate system origin at O_{agg}.

the aggregate represents the average direction of all the long axes of the molecules comprising the aggregate.

For the C_{12}-PDI^+ system, it is assumed that the only nonzero component of the molecular susceptibility tensor is the $\mathbf{T}_{zz}^{mol}$ component, consistent with the dominance of the long-axis polarized transition in this chromophore.[43] It is also assumed that the planar C_{12}-PDI^+ chromophores comprising the aggregate align parallel to one another locally but that the distribution in ϕ is random on larger length scales. Finally, it is assumed that the aggregate X and Z axes lie in the film plane and that the incident longitudinal (Y-polarized) fields in the excitation volume are sufficiently small that they can be neglected.[45] Under these assumptions, the following expression describing the polarization dependence of fluorescence excitation is obtained by expansion of eqs 2 and 3:

$$I_{fl}(\gamma) \propto \langle\cos^4\theta\rangle\cos^4\gamma + \frac{3}{8}\langle 1 - 2\cos^2\theta + \cos^4\theta\rangle\sin^4\gamma + \frac{3}{4}\langle\cos^2\theta - \cos^4\theta\rangle\sin^2 2\gamma \quad (4)$$

Here, γ is the incident polarization (i.e., the angle between the aggregate Z-axis and the incident polarization vector). The brackets in eq 4 indicate that the signal represents an average over the entire distribution of molecular orientations probed.

Fitting of the polarization data to eq 4 provides estimates of $\langle\cos^2\theta\rangle$ and $\langle\cos^4\theta\rangle$, two moments of the in-plane orientation distribution function for the C_{12}-PDI^+ chromophores in the composite thin films. Averages of these parameters, obtained from several different sites such as those shown in Figure 7, yield 0.39 ± 0.02 and 0.25 ± 0.02 for $\langle\cos^2\theta\rangle$ and $\langle\cos^4\theta\rangle$, respectively. These values can be used to obtain estimates of the second ($\langle P_2(\cos^2\theta)\rangle$, or s) and fourth ($\langle P_4(\cos^2\theta)\rangle$) Legendre polynomials more commonly employed as order parameters. Here, the average values for these parameters are +0.09 and +0.01, respectively. While these values only reflect the in-plane order of the samples, if intermolecular interactions within the composite are the dominant factors in determining material organization, chromophores aligned with their long axes perpendicular to the plane of the sample should exhibit a similar level of organization. Hence, these parameters represent a good estimate of overall chromophore order. Their relatively small values are indicative of a high degree of disorder on short-length scales. Such disorder may arise from variations in the alignment of the chromophores or it may result from a mixture of different organizational structures within the films. In future publications, polarization-dependent MPEFM methods will be used to characterize C_{12}-PDI^+ order in samples prepared under conditions meant to alter/enhance chromophore organization.

Conclusions

Photoactive polyelectrolyte surfactant composites incorporating new asymmetrically substituted perylene diimide surfactants have been introduced and characterized by X-ray scattering and optical microscopy. These PE-surf composites show strong evidence of chromophore aggregation via both blue-shifted excitation and absorption spectra for the perylene diimides as well as a dramatic red-shift in their fluorescence emission. The latter was concluded to arise ultimately from excimers whose formation is facilitated by the close association of the perylene diimide cations with the oppositely charged polyelectrolyte. Small-angle X-ray scattering data depict the presence of relatively long-range organization of the molecular components in thin films prepared from these composites but little angstrom-scale order. On longer distance scales, evidence for bilayers having 3.9-nm repeat distances was obtained from the C_{12}-PDI^+/PA^- composites. Multiphoton-excited fluorescence microscopy was employed to characterize overall film morphology and to obtain information on chromophore organization in submicrometer sized domains. The polarization-dependent MPEFM data, taken together with the SAXS data, are consistent with the formation of relatively disordered structures. This disorder may result simply from the randomization of the chromophore alignment, from the presence of different organizational polymorphs, or from the presence of chemically different composite structures. Future studies will further address such issues in these materials by employing annealing methods and different perylene diimide surfactants to control/alter the overall film organization. Over the long term, these new materials should prove useful as alternatives to existing organic semiconductors.

Acknowledgment. The authors thank professors Christer B. Aakeroy, Maryanne M. Collinson, Mark D. Hollingsworth, Duy H. Hua, and Stefan Kraft, all of the Department of Chemistry, Kansas State University, for helpful discussions related to the synthesis and characterization of these materials. The National Science Foundation (CHE-9709034 and CHE-0404578) and the Office of Naval Research (N00014-02-1-0584) are thanked for their support.

LA0471700

(45) Sick, B.; Hecht, B.; Novotny, L. *Phys. Rev. Lett.* **2000**, *85*, 4482.